ANESTHESIOLOGY

Transient Receptor Potential Cation Channels and Calcium Dyshomeostasis in a Mouse Model Relevant to Malignant Hyperthermia

Jose Rafael Lopez, M.D., Ph.D., Vikas Kaura, M.D., Phillip Hopkins, M.D., Xiaochen Liu, Ph.D., Arkady Uryach, M.D., Ph.D., Jose Adams, M.D., Paul D. Allen, M.D., Ph.D

ANESTHESIOLOGY 2020; 133:364–76

EDITOR'S PERSPECTIVE

What We Already Know about This Topic

- The type 1 ryanodine receptor gene (*RYR1*) encoding the skeletal muscle sarcoplasmic reticulum Ca^{2+} release channel is the primary locus for malignant hyperthermia
- Muscle expressing malignant hyperthermia-*RYR1* mutations has chronically elevated intracellular resting calcium and sodium concentrations that increase several-fold on exposure to halothane or isoflurane

What This Article Tells Us That Is New

- The hypothesis that transient receptor potential cation channels play a critical role in causing intracellular calcium and sodium overload in malignant hyperthermia susceptible muscle was tested in a *RYR1*-p.G2435R knock-in murine model of malignant hyperthermia
- Skeletal muscle of mice expressing *RYR1*-p.G2435R had a significantly enhanced, extracellular Ca^{2+}-dependent response to TRPC3/6 channel activators
- The TRPC3/6 channel activator response could be prevented by TRPC3/6 channel blockers
- Local administration of TRPC channel blockers during an active malignant hyperthermia crisis demonstrated that most of the rise in intracellular resting calcium in skeletal muscle comes from the extracellular space and not sarcoplasmic reticulum stores

ABSTRACT

Background: Until recently, the mechanism for the malignant hyperthermia crisis has been attributed solely to sustained massive Ca^{2+} release from the sarcoplasmic reticulum on exposure to triggering agents. This study tested the hypothesis that transient receptor potential cation (TRPC) channels are important contributors to the Ca^{2+} dyshomeostasis in a mouse model relevant to malignant hyperthermia.

Methods: This study examined the mechanisms responsible for Ca^{2+} dyshomeostasis in *RYR1*-p.G2435R mouse muscles and muscle cells using calcium and sodium ion selective microelectrodes, manganese quench of Fura2 fluorescence, and Western blots.

Results: *RYR1*-p.G2435R mouse muscle cells have chronically elevated intracellular resting calcium and sodium and rate of manganese quench (homozygous greater than heterozygous) compared with wild-type muscles. After exposure to 1-oleoyl-2-acetyl-*sn*-glycerol, a TRPC3/6 activator, increases in intracellular resting calcium/sodium were significantly greater in *RYR1*-p.G2435R muscles (from 153 ± 11 nM/10 ± 0.5 mM to 304 ± 45 nM/14.2 ± 0.7 mM in heterozygotes $P < 0.001$] and from 251 ± 25 nM/13.9 ± 0.5 mM to 534 ± 64 nM/20.9 ± 1.5 mM in homozygotes [$P < 0.001$] compared with 123 ± 3 nM/8 ± 0.1 mM to 196 ± 27 nM/9.4 ± 0.7 mM in wild type). These increases were inhibited both by simply removing extracellular Ca^{2+} and by exposure to either a nonspecific (gadolinium) or a newly available, more specific pharmacologic agent (SAR7334) to block TRPC6- and TRPC3-mediated cation influx into cells. Furthermore, local pretreatment with SAR7334 partially decreased the elevation of intracellular resting calcium that is seen in *RYR1*-p.G2435R muscles during exposure to halothane. Western blot analysis showed that expression of TRPC3 and TRPC6 were significantly increased in *RYR1*-p.G2435R muscles in a gene–dose–dependent manner, supporting their being a primary molecular basis for increased sarcolemmal cation influx.

Conclusions: Muscle cells in knock-in mice expressing the *RYR1*-p.G2435R mutation are hypersensitive to TRPC3/6 activators. This hypersensitivity can be negated with pharmacologic agents that block TRPC3/6 activity. This reinforces the working hypothesis that transient receptor potential cation channels play a critical role in causing intracellular calcium and sodium overload in malignant hyperthermia–susceptible muscle, both at rest and during the malignant hyperthermia crisis.

(ANESTHESIOLOGY 2020; 133:364–76)

Malignant hyperthermia is an autosomal dominant hypermetabolic condition triggered by volatile anesthetics and depolarizing neuromuscular blockers.[1] The malignant hyperthermia crisis is characterized by hypercapnia, tachycardia, hypoxemia, muscle rigidity, hypermetabolism, respiratory and metabolic acidosis, and hyperthermia. Human malignant hyperthermia–susceptible individuals appear for the most part to remain subclinical until challenged with pharmacologic triggering agents.[1–3] Once the syndrome is triggered, if left untreated, the mortality of a

Part of the work presented in this article has been presented as a poster at the 63rd Annual Meeting of the Biophysical Society in Baltimore, Maryland, March 2–6, 2019. J.R.L. and V.K. contributed equally to this article.

Submitted for publication December 26, 2019. Accepted for publication April 28, 2020. Published online first on June 5, 2020. From the Department of Molecular Biosciences, School of Veterinary Medicine, University of California at Davis, Davis, California (J.R.L., P.D.A.); the Department of Research (J.R.L.) and the Division of Neonatology (A.U., J.A.), Mount Sinai Medical Center, Miami, Florida; and the Malignant Hyperthermia Investigation Unit, St. James' University Hospital, Leeds, United Kingdom (V.K., P.H., X.L., P.D.A.).

 Anesthesiology 2020; 133:364–76. DOI: 10.1097/ALN.0000000000003387

fulminant malignant hyperthermia episode is higher than 70%, but availability of dantrolene has reduced the mortality to less than 8%.[1,2] Molecular genetic studies have established the type 1 ryanodine receptor gene (*RYR1*) encoding the skeletal muscle sarcoplasmic reticulum Ca^{2+} release channel as the primary locus for malignant hyperthermia.[3–6] More than 200 *RYR1* mutations found throughout the gene have been associated with malignant hyperthermia.[6] To date, one spontaneously occurring porcine model (p.R615C) and four murine knock-in models expressing the murine equivalent of human (p.R163C,[7] p.Y522S,[8] p.G2434R,[9] and p.T4826I[10]) *RYR1* mutations have been studied in detail. All five models exhibit fulminant anesthetic-triggered malignant hyperthermia episodes and heat intolerance with varying gene–dose relationships. The *RYR1*-p.G2435R variant, which is the focus of this study, is a model for the most frequent variant associated with malignant hyperthermia in the United Kingdom and North America. In addition, this is the most common *RYR1* variant to be associated with familial genotype–phenotype discordance.[11] It is associated with a relatively weak *in vitro* contracture test phenotype and is less likely to be associated with an elevated serum creatine kinase compared with p.T4826I and p.R163C.[12,13]

The exact molecular mechanisms by which *RYR1* mutations confer malignant hyperthermia susceptibility are unknown. A common characteristic of muscle expressing malignant hyperthermia-*RYR1* mutations compared with nonsusceptible muscle is an increased resting intracellular calcium concentration in humans[14] and animal models.[15–18] We have shown that exposure to halothane or isoflurane at clinically relevant concentrations causes intracellular calcium concentration to rise several-fold in malignant hyperthermia muscle in experimental animal models, whereas exposure to the same concentrations of halothane or isoflurane had no effect in nonsusceptible muscle.[17,19,20]

Until recently, the mechanism for the malignant hyperthermia crisis has been attributed solely to massive self-sustaining release of Ca^{2+} from the sarcoplasmic reticulum on exposure to triggering agents. Counter to this view, we have introduced a new paradigm that implicates nonspecific sarcolemmal cation entry channels as the predominant source of acute elevations in both intracellular calcium concentration and intracellular sodium concentration during fulminant malignant hyperthermia and are significant contributors to chronically elevated intracellular calcium concentration and intracellular sodium concentration in quiescent malignant hyperthermia-susceptible muscles.[21,22]

The aim of the current study was to use newly available more specific pharmacologic agents and physiologic studies to probe transient receptor potential cation channel (TRPC) function, allowing us to refine their importance in initiating and supporting the malignant hyperthermia crisis in response to triggering agents and with these new data test the hypothesis that TRPCs play a major role in the Ca^{2+} dyshomeostasis that we recently described in a *RYR1*-p.G2435R knock-in murine model of malignant hyperthermia[9] similar to our previous observations in the *RYR1*-p.R163C mouse.[21,22]

Material and Methods

Animals

The animals used in this study were housed in pathogen-free conditions with free access to food and water and 12-h light-and-dark cycles. All experiments were undertaken with approval from the United Kingdom Home Office, the University of California at Davis Institutional Animal Care and Use Committee, or the Mount Sinai Hospital Institutional Animal Care and Use Committee. For single fiber and *in vivo* studies, a mixture of male and female mice between 12 and 16 weeks of age were used, and for myotube studies, myoblasts were isolated from 3- to 5-week-old neonatal mice. All experiments were terminal. For *in vivo* experiments, the malignant hyperthermia animals were allowed to succumb to isoflurane anesthesia when this was used; otherwise they and all wild-type animals were euthanized by cervical dislocation. For muscle collection, all animals were euthanized by cervical dislocation immediately before dissection. Because homozygous animals were viable, the animals were obtained and allocated to homozygous and heterozygous experimental groups by selective breeding of homozygous females to either homozygous or wild-type C57BL/6J males. The animals were used as available in the breeding colony when they reached the appropriate age. Studies on wild-type mice were done on 3- to 5-month-old C57BL/6J animals purchased from Charles River Laboratories (USA) or the St. James's animal facility (United Kingdom) as needed.

Experimental Preparation

The experiments were conducted at room temperature (~23°C): (1) *in vitro* using flexor digitorum brevis muscle fibers from 3- to 5-month-old C57BL/6J (wild-type), heterozygous *RYR1*-p.G2435R, and homozygous *RYR1*-p.G2435R mice: single fibers were obtained by enzymatic digestion as described previously[21]; (2) *in vivo*, in vastus lateralis fibers in wild-type and *RYR1*-p.G2435R mice anesthetized with ketamine/xylazine (100/5 mg/kg body weight) as described previously[22]; and (3) *in vitro* using myotubes differentiated from myoblasts from C57BL/6 (wild-type), *RYR1*-p.G2435R heterozygous, and *RYR1*-p.G2435R homozygous mice as described in detail previously.[9]

Preparation of Calcium and Sodium Selective Microelectrodes

Double-barreled calcium and sodium selective microelectrodes were prepared as described previously.[14,22] Each ion-selective microelectrode was individually calibrated

before and after the determination of intracellular calcium concentration and intracellular Na^+ concentration as described before.[22] Only those Ca^{2+}-selective microelectrodes with a linear relationship between pCa 3 and 7 (Nernstian response, 29.5 and 30.5 mV/pCa unit at 23 and 37°C, respectively) were used experimentally. The Na^+-selective microelectrodes gave virtually Nernstian responses at free sodium concentrations between 100 and 10 mM. However, although at concentrations between 10 and 1 mM Na^+, the electrodes had a sub-Nernstian response (40 to 45 mV), their response was of a sufficient amplitude to be able to measure intracellular sodium concentration. The sensitivity and response of the calcium- and sodium-selective microelectrodes were not directly affected by any of the drugs used in the present study.

Calcium and Sodium Determinations in Muscle Fibers

Microelectrode recordings were performed as described previously.[22] Single isolated adult flexor digitorum brevis muscle fibers (*in vitro*) or vastus lateralis muscle fibers (*in vivo*) from wild-type and *RYR1*-p.G2435R heterozygous and homozygous mice were impaled with either double-barreled Ca^{2+} or double-barreled Na^+ -selective microelectrodes, and their potentials were recorded *via* a high-impedance amplifier (WPI Duo 773 electrometer; WPI, USA). The potential from the 3 M potassium chloride microelectrode was subtracted electronically from the potential of either the calcium electrode or the sodium electrode to produce a differential calcium-specific potential or sodium-specific potential that represents the intracellular calcium concentration or intracellular sodium concentration, respectively. All electrode potentials were filtered (30 to 50 kHz) to improve the signal-to-noise ratio and stored in a computer for further analysis. The data from any given electrode impalement were accepted if the 3 M potassium chloride microelectrode potential was greater than or equal to −80mV, and we were able to make a stable recording of both the 3 M potassium chloride microelectrode potential and the calcium or sodium-specific potential for 60 s. These criteria resulted in rejection of data from 20% of *in vivo* impalements and 30 to 35% of *in vitro* impalements. There was no genotype effect on rejection rate.

Measurements of Manganese Quench of Fura2 in Myotubes and Isolated Single Fibers

When the Ca^{2+} indicator Fura2 is exposed to manganese, its fluorescence at its isobestic emission wavelength is quenched. Because TRPC3, TRPC6, Orai1, Orai2, Orai3, and slow voltage-gated Ca^{2+} channels are permeable to manganese as well as Ca^{2+}, the rate of manganese quench can be used to determine the rate of Ca^{2+} entry into a cell.

We used manganese quench to assess sarcolemmal divalent cation entry in myotubes or isolated single adult muscle fibers loaded with 5 μM Fura2-AM for 30 min at 37°C. The solution containing the Fura2-AM was washed off, and the cells were maintained for 25 min at room temperature to allow deesterification and equilibration of the intracellular Fura2. The cells were observed through a 40× 1.3 NA objective on a Nikon Eclipse T2000 epifluorescence microscope using an excitation wavelength of 360 ± 5 nm (the isosbestic wavelength of Fura2 at which the fluorescence of the dye is independent of the Ca^{2+}-free state *vs.* the Ca^{2+}-bound state), and the emission signal was measured at 510 ± 40 nm. Images were captured with 2 × 2 binning at a rate of 5 frames/s using an intensified 12-bit digital intensified charge-coupled device (ORCA-ER) and IPLab software. Regions of interest in individual cells were analyzed using ImageJ software (National Institutes of Health), with the data exported to GraphPad Prism 7. Prism was used to fit linear regression models (y = mx + c) for the basal signal in imaging buffer and then independently in manganese-containing solutions with and without treatment drugs. The specific rate of Fura2 quenching induced by manganese entry was calculated by subtracting the basal slope of decline of fluorescence over time from the slope during the application of manganese buffer (*i.e.*, net slope) and is expressed as arbitrary fluorescence units/s. The net slope was calculated in the absence and presence of treatment drugs. Cells with a positive net slope after the addition of manganese buffer were excluded from analysis because this indicated a technical problem with the measurement. For the same reason the slope of the quench signal was normalized to 0 when the net slope was positive after treatment with a cation channel antagonist.

Western Blot Analysis of TRPC3 and TRPC6 Expression. Gastrocnemius muscles from all genotypes were dissected, minced, and homogenized in modified radioimmunoassay precipitation assay buffer. Total protein concentration was determined using the bicinchoninic acid method (Thermo Scientific, USA). Samples of whole gastrocnemius homogenate were prepared as described by Altamirano *et al.*[21] and incubated overnight at 4°C with primary antibodies: rabbit anti–transient receptor potential cation channel 3 (TRPC3), dilution 1:2,500 (ab51560; Abcam, USA), rabbit anti-TRPC6, dilution 1:2,500 (ab62461; Abcam), human anti-actin, dilution of 1:5,000 (SC8432; Santa Cruz, USA). All of these antibodies have been validated previously by different research groups and our laboratory. The resolved bands were detected with a Storm 860 imaging system (GE Bio-Sciences, USA). The protein levels were quantified using myImageAnalysis software (Thermo Fisher Scientific, USA) and normalized to β-actin.

Solutions

The mammalian Ringer solution used for experiments using muscle fibers had the following composition: 140 mM NaCl, 5 mM KCl, 2 mM $CaCl_2$, 1 mM $MgCl_2$, 5 mM glucose, and 10 mM HEPES, pH 7.4. The imaging buffer used for the experiments with myotubes contained 133 mM

NaCl, 5 mM KCl, 2 mM $CaCl_2$, 1 mM $MgCl_2$, 5.5 mM glucose, and 10 mM HEPES, pH 7.4. In the manganese buffer, the $CaCl_2$ and $MgCl_2$ were substituted with 0.5 mM $MnCl_2$. The Ca^{2+}-free solution had the following composition: 140 mM NaCl, 5 mM KCl, 2 mM $MgCl_2$, 1 mM EGTA, 5 mM glucose, and 10 mM HEPES, pH 7.4. 1-Oleoyl-2-acetyl-*sn*-glycerol, gadolinium, SAR7334, and hyperforin solutions were made by adding the desired concentration of the reagent to the physiologic or manganese-containing solutions.

Statistics

Neither randomization nor blinding of the investigator performing the test was used for these studies. No specific power calculation was conducted before experimentation, but the rationale for the sample sizes used was based on our previous studies using this and other animal models of malignant hyperthermia with the same and different pharmacologic interventions. All values of intracellular ion concentrations are expressed as means ± SD, with N_{mice} representing the number of mice used to collect muscle fibers or used for the *in vivo* experiments and N_{fibers} representing the number of myotubes or muscle fibers in which measurements were carried out. Statistical analysis for studies done on muscle fibers both *in vitro* and *in vivo* was performed using one-way between-genotypes ANOVA with Tukey *post hoc* test for multiple measurements to determine significance. The results of Western blots were analyzed using Student's unpaired independent *t* test. Normal distribution of the data was verified by histogram analysis. For studies of manganese quench in myotubes, the results were not normally distributed and therefore are expressed as the median and interquartile range. These results were analyzed using a Kruskal–Wallis test with Dunn's multiple comparison to determine significance. $P < 0.05$ was accepted as the minimum confidence level for significance for all comparisons, but the *P* values obtained for each comparison are reported. With the exception of the myotube manganese quench studies, in which positive quench data were excluded or normalized to zero as described above, and muscle fiber data, in which the criteria for a successful measurement was not met (based on either a depolarized membrane potential or lack of stable electrode recording for 60 s), no outlying data were removed from the data collected before or after analysis. All statistical analyses were performed using GraphPad Prism 7 software.

Results

Resting Intracellular Calcium and Sodium Concentrations

Malignant hyperthermia is characterized by an intracellular Ca^{2+} and Na^+ dyshomeostasis.[14,19,22,23] Consequently, intracellular calcium concentration or intracellular sodium concentration was measured in quiescent single muscle fibers isolated from wild-type, *RYR1*-p.G2435R heterozygous, and *RYR1*-p.G2435R homozygous cells using double-barreled ion-specific microelectrodes. The intracellular calcium concentration was 120 ± 2 nM (N = 8) in wild-type mice, whereas it was 156 ± 11 nM (N = 11) in *RYR1*-p.G2435R heterozygous and 275 ± 15 nM (N = 10) in homozygous ($P < 0.001$ for both; fig. 1A) mice. Likewise, intracellular sodium concentration was more elevated in *RYR1*-p.G2435R heterozygous and homozygous fibers than that observed in wild-type fibers. The intracellular sodium concentration was 8 ± 0.1 mM (N = 8) in wild-type fibers, whereas it was 10 ± 1 mM (N = 9) in *RYR1*-p.G2435R heterozygotes and 14 ± 0.6 mM (N = 11) in *RYR1*-p.G2435R homozygotes, respectively ($P < 0.001$ for both; fig. 1A). The resting membrane potentials were not different among genotypes (−82 ± 1.2 mV [N = 29] in resting wild-type muscle fibers, −82 ± 1.3mV [N = 31] in *RYR1*-p.G2435R heterozygous muscle fibers, and −1 ± 2.3 mV [N = 34] in *RYR1*-p.G2435R homozygous muscle fibers).

As previously reported, similar differences for intracellular calcium concentration and intracellular sodium concentration were obtained in the *in vivo* measurements carried out on the vastus lateralis from wild-type and malignant hyperthermia mice.[9] In a new data set carried out for this study, intracellular calcium concentration in wild-type mice was 122 ± 3 nM (N = 15) compared with 144 ± 9 nM (N = 14) and 259 ± 31 nM (N = 18) in *RYR1*-p.G2435R heterozygous and *RYR1*-p.G2435R homozygous muscles, respectively (fig. 1B). Intracellular sodium concentration was 8 ± 0.1 mM (N = 16) in wild-type mice compared with 9.5 ± 1 mM (N = 16) and 12.9 ± 1.5 mM (N = 13) in *RYR1*-p.G2435R heterozygous and *RYR1*-p.G2435R homozygous muscles, respectively ($P < 0.001$ compared with wild-type muscles; fig. 1B). Taken together, the results demonstrate that there is a comparable intracellular calcium and sodium overload in both isolated *RYR1*-p.G2435R muscle cells and intact muscle fibers compared with wild-type muscle fiber and that resting intracellular ion recordings under *in vitro* conditions recapitulate those found *in vivo*.

1-Oleoyl-2-acetyl-*sn*-glycerol Induces an Elevation of Intracellular Calcium and Sodium Concentrations

To directly investigate the effect of diacylglycerol on intracellular calcium and intracellular sodium concentrations, single muscle fibers were exposed to 1-oleoyl-2-acetyl-*sn*-glycerol, a membrane-permeable diacylglycerol analog that has been shown to activate transient receptor potential cation channel subfamily C member 3 (TRPC3) and member 6 (TRPC6) channels.[24] Incubation of muscle fibers in 1-oleoyl-2-acetyl-*sn*-glycerol (100 μM) for 5 min produced an elevation of intracellular calcium concentration in all genotypes. In wild-type mice, the intracellular calcium concentration was increased by 60% (from 123 ±

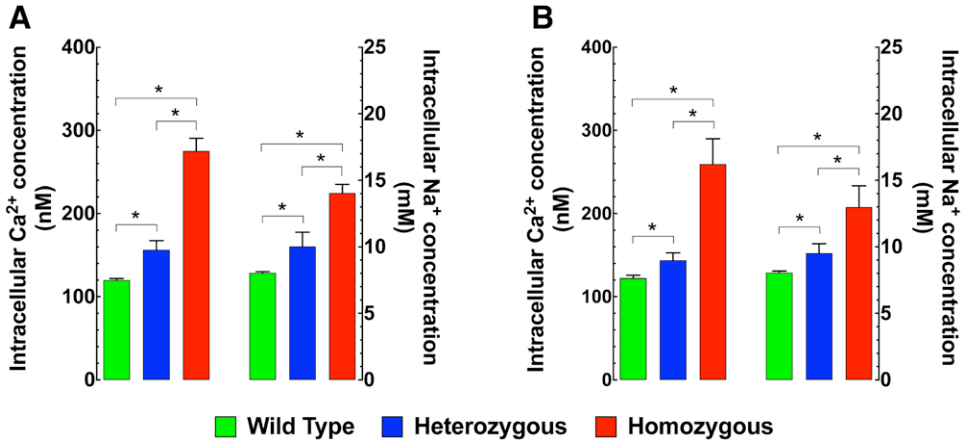

Fig. 1. Elevated intracellular Ca^{2+} and Na^{+} concentrations in *RYR1*-p.G2435R malignant hyperthermia muscle cells. Intracellular Ca^{2+} or Na^{+} concentration was measured in quiescent flexor digitorum brevis fibers isolated from wild-type, *RYR1*-p.G2435R heterozygous, and *RYR1*-p.G2435R homozygous mice (*A*) and *in vivo* from the vastus lateralis fibers in anesthetized wild-type, *RYR1*-p.G2435R heterozygous, and *RYR1*-p.G2435R homozygous mice (*B*) using double-barreled ion-specific microelectrodes. *In vitro*, N_{mice} = 3 per experimental condition, N_{cell} = 15 to 18 per genotype for intracellular Ca^{2+} concentration measurements; N_{mice} = 3 per experimental condition, N_{cell} =15 to 18 per genotype for intracellular Na^{+} concentration measurements. *In vivo*, N_{mice} = 4 per genotype, N_{cell} = 13 to 16 per experimental condition for intracellular Ca^{2+} concentration measurements; N_{mice} = 5 per experimental condition, N_{cell} = 8 to 11 per genotype for intracellular Na^{+} concentration measurements. The values are expressed as means ± SD for each condition; one-way ANOVA with Tukey *post hoc* test. *$P \leq 0.05$.

3 nM [N = 11] to 196 ± 27 nM [N = 13], $P < 0.001$); in *RYR1*-p.G2435R heterozygous fibers, it was enhanced by 99% (from 153 ± 11 nM [N = 12] to 304 ± 45 nM [N = 11], $P < 0.001$); and in *RYR1*-p.G2435R homozygous fibers, it was elevated by 113% (from 251 ± 25 nM [N = 12] to 534 ± 64 nM [N = 13], $P < 0.001$; fig. 2A).

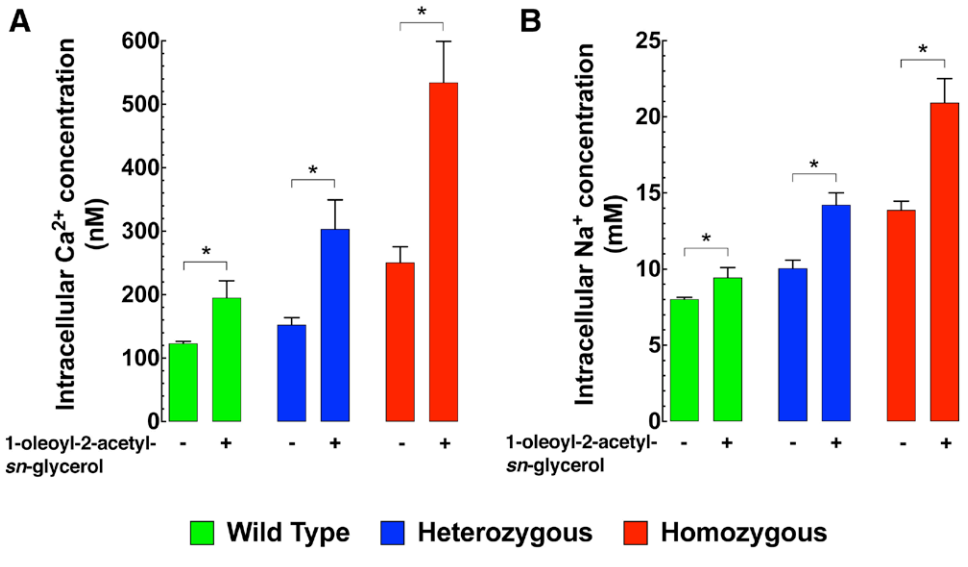

Fig. 2. 1-Oleoyl-2-acetyl-*sn*-glycerol provokes elevation of intracellular Ca^{2+} and Na^{+} concentrations. Exposure of quiescent flexor digitorum brevis fibers to 1-oleoyl-2-acetyl-*sn*-glycerol 100 μM induced an elevation of intracellular Ca^{2+} (*A*) and Na^{+} concentration (*B*) that was greater in *RYR1*-p.G2435R fibers (homozygous greater than heterozygous) than wild-type muscle fibers. Over the *horizontal axis* are indicated the experimental conditions. For intracellular Ca^{2+} concentration measurements, N_{mice} = 3 per experimental condition, N_{cell} = 11 to 13 per genotype. For intracellular Na^{+} concentration measurements, N_{mice} = 3 per experimental condition, N_{cell} = 9 to 10 per genotype. The values are expressed as means ± SD for each condition; one-way ANOVA with Tukey *post hoc* test. *$P \leq 0.05$.

Because the permeability of TRPCs is cation-specific but not Ca^{2+}-specific, their activation could also increase sodium entry and intracellular sodium concentration. Application of 1-oleoyl-2-acetyl-*sn*-glycerol (100 μM) significantly elevated intracellular sodium concentration in all genotypes, but its effect was greater in *RYR1*-p.G2435R muscle cells than in wild-type muscle cells (fig. 2B). In wild-type mice, incubation with 1-oleoyl-2-acetyl-*sn*-glycerol elevated intracellular sodium concentration by 18% (from 8 ± 0.1 mM, N = 10 to 9.4 ± 0.7 mM, N = 9, $P < 0.001$), in *RYR1*-p.G2435R heterozygous by 42% (from 10 ± 0.5 mM, N = 10 to 14.2 ± 0.7 mM, N = 9, $P < 0.001$), and in *RYR1*-p.G2435R homozygous by 50% (from 13.9 ± 0.5 mM, N = 9 to 20.9 ± 1.5 mM, N = 10, $P < 0.001$). These elevations of intracellular calcium and sodium concentrations induced by 1-oleoyl-2-acetyl-*sn*-glycerol were not affected by the voltage-gated Ca^{2+} channel inhibitor nifedipine (10 μM) nor associated with changes in resting membrane potential in either wild-type or *RYR1*-p.G2435R muscle fibers (data not shown).

Removal of Extracellular Ca^{2+} Prevented Increases in Intracellular Calcium Concentration Induced by 1-Oleoyl-2-acetyl-*sn*-glycerol

In a different set of experiments, we explored the contribution of the Ca^{2+} influx on intracellular calcium concentration elevation elicited by 1-oleoyl-2-acetyl-*sn*-glycerol. Single wild-type and *RYR1*-p.G2435R muscle fibers were incubated for 5 min in Ca^{2+}-free solution before 1-oleoyl-2-acetyl-*sn*-glycerol (100 μM) treatment. This exposure significantly reduced intracellular calcium concentration in all genotypes but had a greater effect in *RYR1*-p.G2435R mice than in wild-type mice (fig. 3). In wild-type fibers, Ca^{2+}-free solution reduced intracellular calcium concentration from 123 ± 4 nM (N = 10) to 98 ± 6 nM (N = 12, $P < 0.001$), whereas in *RYR1*-p.G2435R heterozygous fibers, it was reduced from 161 ± 26 nM (N = 14) to 136 ± 6 nM (N = 12, $P < 0.001$), and in *RYR1*-p.G2435R homozygous fibers, it decreased from to 256 ± 27 nM (N = 12) to 176 ± 17 nM (N = 14, $P < 0.001$). In addition, the observed rise in intracellular calcium concentration elicited by 1-oleoyl-2-acetyl-*sn*-glycerol was completely inhibited in both wild-type and *RYR1*-p.G2435R muscle fibers in the absence of extracellular Ca^{2+} (fig. 3).

Blocking Sarcolemmal Calcium and Sodium Entry with Gadolinium Abolishes the Increases in Intracellular Calcium and Sodium Concentrations Elicited by 1-Oleoyl-2-acetyl-*sn*-glycerol

To gain further insight into molecular mechanisms for the increased sarcolemmal Ca^{2+} and Na^{+} entry responsible for the elevation in intracellular calcium and sodium concentrations after exposure to 1-oleoyl-2-acetyl-*sn*-glycerol, we measured intracellular calcium concentration and

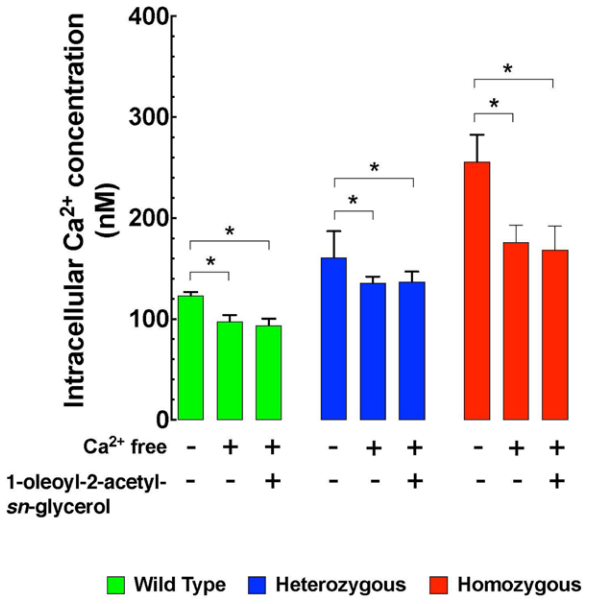

Fig. 3. Removal of extracellular Ca^{2+} prevents the 1-oleoyl-2-acetyl-*sn*-glycerol-induced increase in intracellular Ca^{2+} concentration. Removal of extracellular Ca^{2+} lowered the intracellular Ca^{2+} concentration and provoked the inhibition of 1-oleoyl-2-acetyl-*sn*-glycerol (100 μM)–induced elevation of intracellular Ca^{2+} concentration in flexor digitorum brevis fibers isolated from Wild type, *RYR1*-p.G2435R heterozygous, and *RYR1*-p.G2435R homozygous mice. On the *horizontal axis* are indicated the experimental conditions used. For intracellular Ca^{2+} concentration measurements: N_{mice} = 3 per experimental condition, N_{cell} = 10 to 14 per genotype. Values are expressed as means ± SD for each condition. One-way ANOVA with Tukey *post hoc* test. *$P \leq 0.05$.

intracellular sodium concentration in isolated single wild-type and *RYR1*-p.G2435R muscle fibers before and after incubation in gadolinium and then in the presence of gadolinium, after exposure to 1-oleoyl-2-acetyl-*sn*-glycerol (100 μM). Pretreatment with 25 μM gadolinium significantly lowered intracellular calcium concentration and intracellular sodium concentration by 15% and by 8%, respectively, in wild-type fibers; by 20% by 15%, respectively, in *RYR1*-p.G2435R heterozygous fibers; and by 27% and 29%, respectively, in *RYR1*-p.G2435R homozygous fibers (figs. 4, A and B). Furthermore, gadolinium pretreatment prevented any significant increase in intracellular calcium and sodium concentrations during exposure to 1-oleoyl-2-acetyl-*sn*-glycerol in all genotypes (figs. 4, A and B).

SAR7334 Blocks the Effects of 1-Oleoyl-2-acetyl-*sn*-glycerol

Because gadolinium is a nonspecific sarcolemmal cation blocker, SAR7334, a newer more specific blocker of TRPC6 and TRPC3 channels,[25] was used to further characterize the mechanism for the 1-oleoyl-2-acetyl-*sn*-glycerol–mediated increase in intracellular calcium concentration.

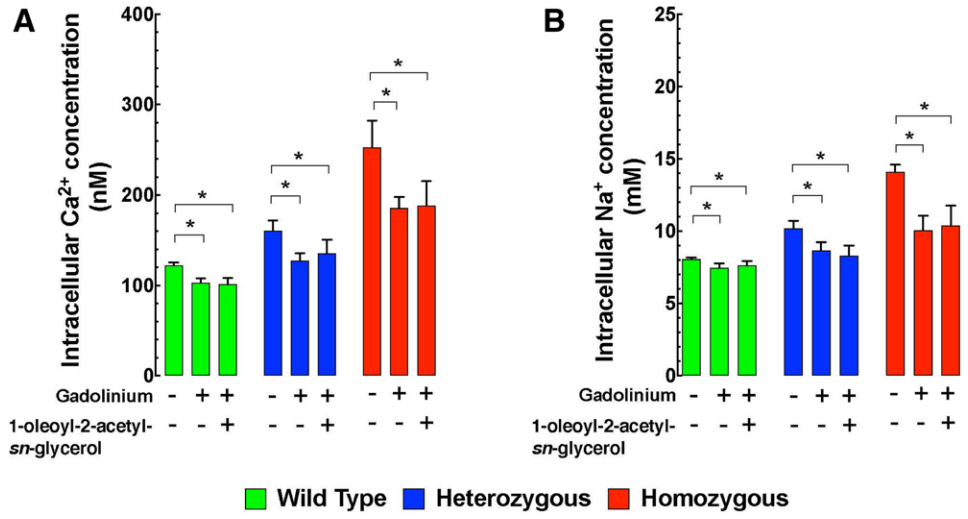

Fig. 4. Gadolinium abolishes the 1-oleoyl-2-acetyl-*sn*-glycerol effects on intracellular Ca^{2+} and Na^{+} concentrations. Preincubation of wild-type, *RYR1*-p.G2435R heterozygous, and *RYR1*-p.G2435R homozygous flexor digitorum brevis fibers in gadolinium (25 μM) reduced the intracellular Ca^{2+} and Na^{+} concentrations and eliminated the increase in intracellular Ca^{2+} (*A*) and Na^{+} concentrations (*B*) induced by 1-oleoyl-2-acetyl-*sn*-glycerol. Over the *horizontal axis* are indicated the experimental conditions used. For intracellular Ca^{2+} determinations, N_{mice} = 4 per experimental condition, N_{cell} = 17 to 19 per genotype. For intracellular Na^{+} determinations, N_{mice} = 4 per experimental condition, N_{cell} = 13 to 15 per genotype. The values are expressed as means ± SD for each condition; one-way ANOVA with Tukey *post hoc* test. *$P \leq 0.05$.

Single isolated wild-type and *RYR1*-p.G2435R muscle fibers were incubated in 1 μM SAR7334 and then exposed to 1-oleoyl-2-acetyl-*sn*-glycerol (100 μM). Pretreatment with SAR7334 significantly reduced the resting intracellular calcium concentration by 14% in wild-type fibers, by 19% in *RYR1*-p.G2435R heterozygous fibers, and by 34% in *RYR1*-p.G2435R homozygous fibers (fig. 5A). Furthermore, SAR7334 also prevented the 1-oleoyl-2-acetyl-*sn*-glycerol–mediated elevation of intracellular calcium concentration in all three genotypes (fig. 5A).

SAR7334 Partially Blocked the Elevation of Intracellular Calcium Concentration Associated with Malignant Hyperthermia Episode

Having observed inhibition of the 1-oleoyl-2-acetyl-*sn*-glycerol–induced increase in intracellular calcium concentration by SAR7334 in wild-type and *RYR1*-p.G2435R single muscle fibers, we then tested the activity of this TRPC3/6 channel blocker during a malignant hyperthermia episode. We therefore investigated the effect of SAR7334 on intracellular calcium concentration in malignant hyperthermia muscle *in vivo* during exposure to 2% halothane. The intracellular calcium concentration was measured simultaneously in the right and left vastus lateralis muscles in wild-type and homozygous *RYR1*-p.G2435R mice before and after the addition of 2% halothane to their inspired gas (fig. 5B). The right vastus lateralis muscle was pretreated locally with 1 μM SAR7334, and the left muscle served as the control. Figure 5B shows a typical *in vivo* experiment carried out in a homozygous *RYR1*-p.G2435R mouse. The data are reported as nanomolar (nM). Before drug treatment, the intracellular calcium concentration was very similar in muscles from both legs (265 ± 9 nM in the left leg *vs.* 275 ± 9 nM in the right leg). Ten minutes after the application of 1 μM SAR7334 on the exposed vastus lateralis fibers of the right leg, the intracellular calcium concentration was reduced from 265 ± 9 to 187 ± 11 nM (fig. 5B). Inhalation of halothane elicited an elevation of intracellular calcium concentration in the untreated leg to 1,373 ± 81 nM, whereas in the SAR7334-treated leg, the initial increase in intracellular calcium concentration was reduced by 62% (526 ± 99 nM), after which intracellular calcium concentration declined to 453 ± 32nM (fig. 5B). After 20 min of inhalation of halothane, the rectal temperature reached 42°C, and the mouse died.

Hyperforin Induced Elevation of Intracellular Calcium and Sodium Concentrations

Hyperforin is known to elevate the intracellular concentration of Ca^{2+} through the activation of di-acyl-glycerol–sensitive TRPC6 channels without activating the other transient receptor potential cation channel isoforms (TRPC1, TRPC3, TRPC4, TRPC5, and TRPC7).[26] Hyperforin (5 μM) caused a prominent sustained rise in intracellular calcium concentration that was greater in *RYR1*-p.G2435R fibers (homozygous greater than heterozygous)

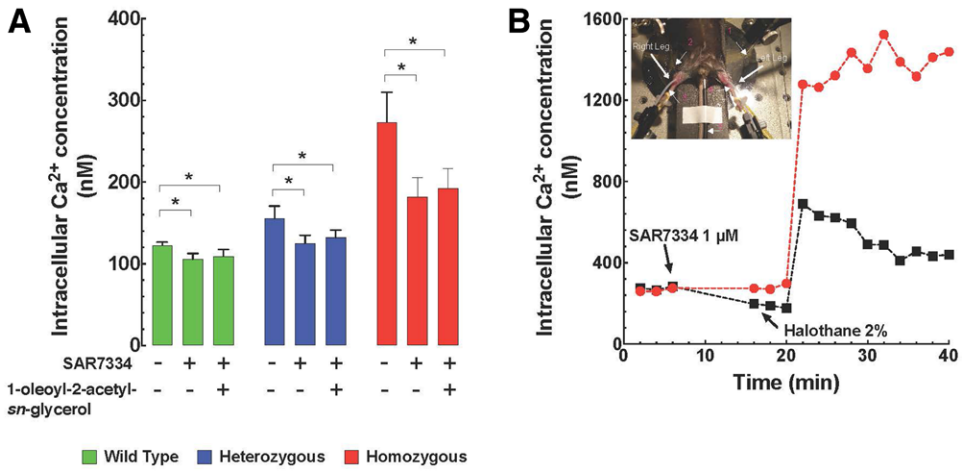

Fig. 5. SAR7334 blocked the elevation of intracellular Ca^{2+} concentration induced by 1-oleoyl-2-acetyl-*sn*-glycerol and partially inhibited the increase associated with a malignant hyperthermia episode. Intracellular Ca^{2+} concentration was measured in wild-type, *RYR1*-p.G2435R heterozygous, and *RYR1*-p.G2435R homozygous flexor digitorum brevis fibers before and after incubation in SAR7334 (1 μM), as well as after the incubation in SAR7334 when exposed to 1-oleoyl-2-acetyl-*sn*-glycerol (100 μM). (*A*) Preincubation in SAR7334 reduced intracellular Ca^{2+} concentration in all genotypes and prevented the increase in intracellular calcium concentration induced by 1-oleoyl-2-acetyl-*sn*-glycerol. Over the *horizontal axis* are indicated the experimental conditions. (*B*) Typical experiment carried out *in vivo* in *RYR1*-p.G2435R homozygous mice anesthetized with 100 mg/kg ketamine and 50 mg/kg xylazine. Intracellular calcium concentration was measured simultaneously in the superficial fibers of the vastus lateralis muscle in the right and left hind limb. Superficial muscle fibers were superfused with Ringer solution alone (left leg, control, *red line*) or SAR7334 (1 μM) for 5 min (right leg, *black line*), and the mouse was then exposed to 2% halothane by inhalation (*black arrow*). The *inset* in the *left upper corner* shows the experimental arrangement. *Arrows 1* and *2*, Ca^{2+} microelectrodes; *arrows 3* and *4*, grounds; *arrow 5*, rectal temperature probe. For intracellular Ca^{2+} concentration measurements in (*A*), $N_{mice} = 4$ per genotype, $N_{cell} = 13$ to 18 per experimental condition. The values are expressed as means ± SD for each condition; one-way ANOVA with Tukey *post hoc* test. *$P \leq 0.05$.

than wild-type muscle fibers (fig. 6A). In wild-type muscle fibers, intracellular calcium concentration was enhanced from 124 ± 3 nM (N = 9) to 151 ± 10 nM (N = 10) upon incubation with hyperforin, whereas in *RYR1*-p.G2435R heterozygous fibers, it increased from 164 ± 22 nM (N = 10) to 234 ± 31 nM (N = 10), and in *RYR1*-p.G2435R homozygous fibers, it was elevated from 269 ± 37 nM (N = 10) to 441 ± 41 nM (N = 10; fig. 6A). Removal of extracellular Ca^{2+} reduced pre-exposure intracellular calcium concentration and blocked the hyperforin effect in all genotypes (fig. 6C). Similar to its effect on intracellular calcium concentration, hyperforin elevated intracellular sodium concentration in wild-type fibers from 8 ± 0.1 mM (N = 15) to 9.5 ± 0.6 mM (N = 10; $P < 0.001$), in *RYR1*-p.G2435R heterozygous fibers from 10 ± 0.6 mM (N = 15) to 13.5 ± 1 (N = 10; $P < 0.001$), and in *RYR1*-p.G2435R homozygous fibers from 14.5 ± 1.2 mM (N = 11) to 20.3 ± 1.6 mM (N = 13; $P < 0.001$; fig. 6B).

Effects of Genotype and Sarcolemmal Cation Entry Agonists and Antagonists on Manganese Quench of Fura2 in Differentiated Myotubes. When the buffer was changed from imaging buffer to manganese quench buffer, baseline quench of Fura2 fluorescence was observed in all three genotypes (fig. 7A for representative traces reported as arbitrary fluorescence units) with the median quench rate being greater in malignant hyperthermia–homozygous (−0.23 arbitrary fluorescence units/s; interquartile range, −0.13 to −0.38 arbitrary fluorescence units/s) *versus* malignant hyperthermia–heterozygous (−0.18 arbitrary fluorescence units/s; interquartile range, −0.11 to −0.32 arbitrary fluorescence units/s) and wild-type mice (−0.19 arbitrary fluorescence units/s; interquartile range, −0.12 to −0.32 arbitrary fluorescence units/s; fig. 7B). Qualitatively similar results were observed in isolated adult single muscle fibers (data not shown).

We next determined the effect of sarcolemmal cation blockers 25 μM gadolinium (a nonspecific sarcolemmal cation entry blocker) and 250 nM SAR7334 (a transient receptor potential cation channel specific blocker) on the rate of manganese quench of the Fura2 fluorescence signal. Treatment with 25 μM gadolinium profoundly blocked manganese quench to near baseline levels in all three genotypes ($P < 0.0001$, N = 65 to 96; fig. 7B). The reduction in the median quench rate was 88% in wild-type myotubes (N = 65), 100% in heterozygous *RYR1*-p.G2435R myotubes (N = 72), and 95.6% in homozygous *RYR1*-p.G2435R myotubes (N = 96; fig. 7B). After treatment with 250 nM SAR7334 in wild-type myotubes, the change in median quench rate was not significant (8%, $P > 0.999$, N = 49), whereas in heterozygous

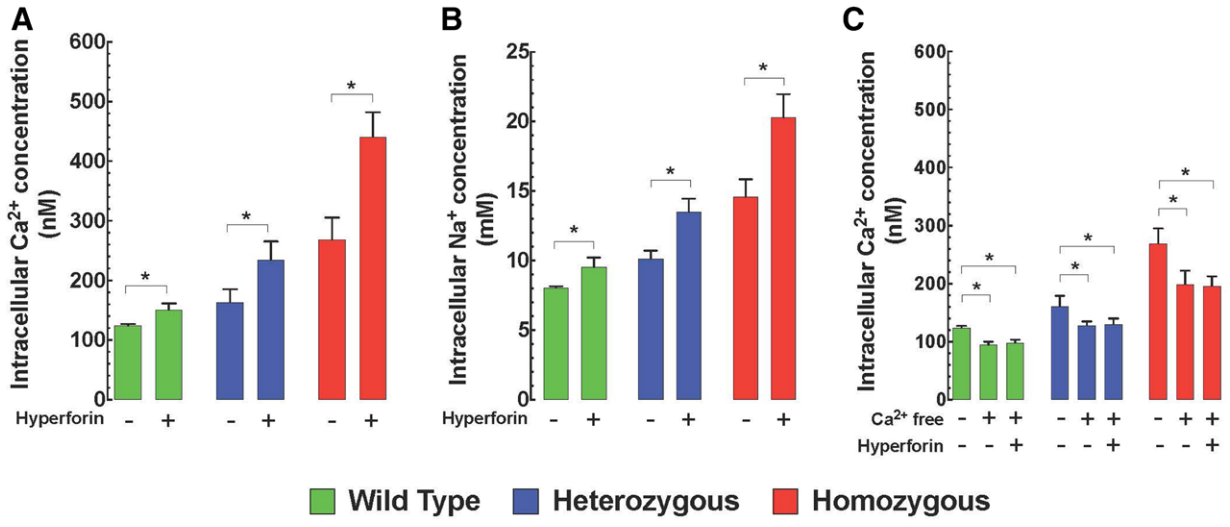

Fig. 6. Effect of hyperforin on intracellular Ca^{2+} and Na^{+} concentrations. Hyperforin (5 μM) caused a sustained rise in intracellular Ca^{2+} and Na^{+} concentration in single flexor digitorum brevis muscle fibers that were greater in *RYR1*-p.G2435R mice (homozygous greater than heterozygous) than in wild-type mice (*A* and *B*). Removal of extracellular Ca^{2+} inhibited the hyperforin effect on intracellular Ca^{2+} concentration (*C*). On the *horizontal axes* are indicated the experimental conditions. For intracellular Ca^{2+} concentration determinations in (*A*), N_{mice} = 3 per experimental condition, N_{cell} = 9 to 10 per genotype. For intracellular Na^{+} concentration determinations in (*B*), N_{mice} = 3 per experimental condition, N_{cell} = 10 to 15 per genotype. For intracellular Ca^{2+} concentration determinations in (*C*), N_{mice} = 3 per experimental condition, N_{cell} = 10 to 12 per genotype. The values are expressed as means ± SD for each condition; paired and unpaired *t* test and one-way ANOVA with Tukey *post hoc* test. *$P \leq 0.05$.

RYR1-p.G2435R myotubes and in homozygous *RYR1*-p.G2435R myotubes, there was a significant decrease (45%, $P < 0.005$, N = 53 and 69%, $P < 0.001$, N = 35 for heterozygous and homozygous *RYR1*-p.G2435R myotubes, respectively) in the median manganese quench rate (fig. 7B).

Protein Expression Differences in Wild-type and RYR1-p.G2435R Muscle. Western blot analysis showed that TRPC3 and TRPC6 were significantly increased in a gene–dose–dependent manner in *RYR1*-p.G2435R muscles (heterozygous [$P < 0.01$] and homozygous [$P < 0.001$]) compared with wild-type mice. Figure 8A shows representative Western blot analysis of the expression of TRPC3 and TRPC6 in wild-type, heterozygous *RYR1*-p.G2435R, and homozygous *RYR1*-p.G2435R muscle; β-actin was used as a loading control. Densitometric analysis of five independent Western blots for each transient receptor potential cation channel protein is shown in figure 8B.

Discussion

The major findings of the present study are as follows.

(1) We confirmed our previous finding[9] that *RYR1*-p.G2435R muscle cells have chronically elevated intracellular resting calcium and sodium concentrations (greater in homozygous than in heterozygous mice) and now show that this is associated with elevated manganese quench indicating increased sarcolemmal cation influx.

(2) Compared with wild-type muscle cells, incubation of *RYR1*-p.G2435R muscle cells with 1-oleoyl-2-acetyl-*sn*-glycerol or the TRPC6 activator hyperforin significantly increased intracellular calcium and sodium concentrations (greater in homozygous than heterozygous muscle cells).

(3) Increases in intracellular calcium and sodium concentrations induced by 1-oleoyl-2-acetyl-*sn*-glycerol are dependent on extracellular Ca^{2+} and are blocked by the nonspecific sarcolemmal cation channel blocker gadolinium, as well as the more specific TRPC3 and TRPC6 channel blocker SAR7334.

(4) SAR7334 treatment also significantly reduced resting intracellular calcium and sodium concentrations, blocked manganese quench, and reduced the elevation of intracellular calcium in *RYR1*-p.G2435R fibers after exposure to halothane.

(5) The observed changes in the above *RYR1*-p.G2434R responses were accompanied by an increase in the protein expression of TRPC3 and TRPC6 in *RYR1*-p.G2435R (homozygous greater than heterozygous) skeletal muscles compared with wild-type muscles.

For some time, it has been thought that the mechanism behind the increased resting intracellular calcium in malignant hyperthermia susceptible muscle is simply due to sarcoplasmic reticulum leak and that the massive increase in muscle intracellular calcium during an

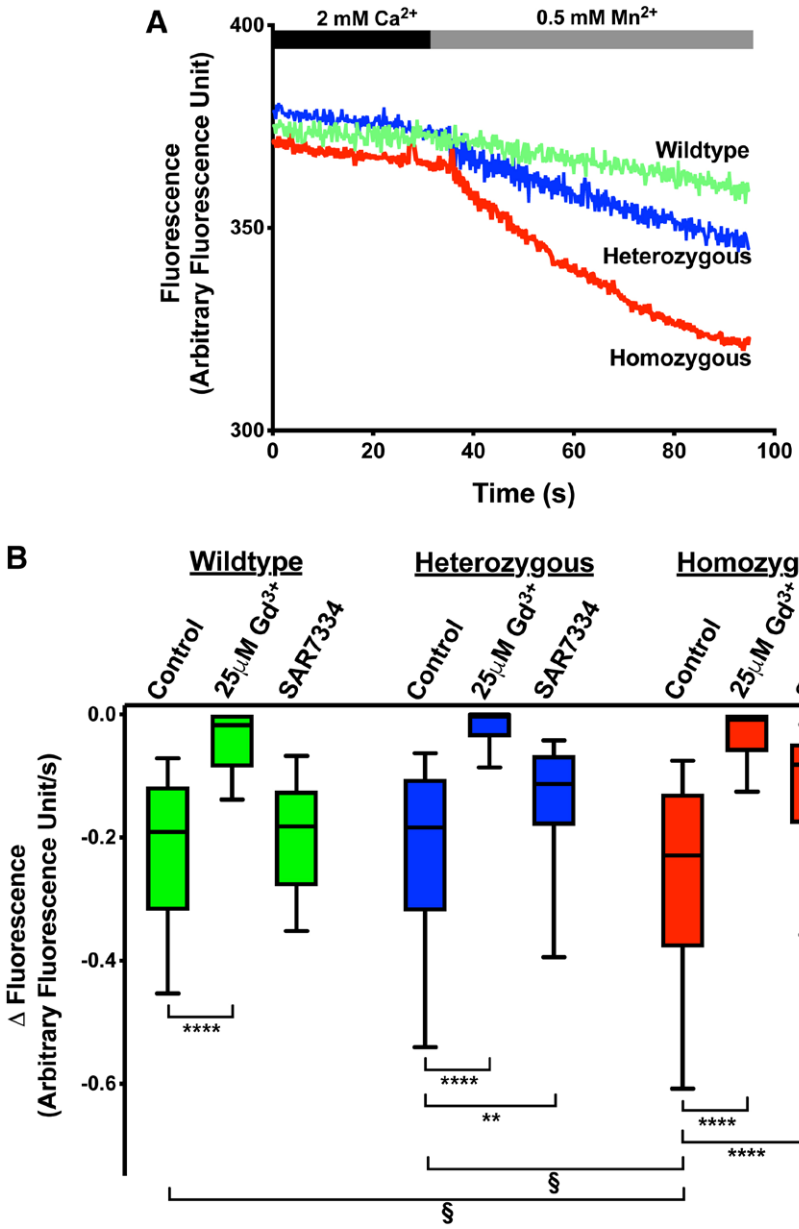

Fig. 7. Resting sarcolemmal divalent cation permeability in myotubes. (*A*) Representative traces indicating the change in the rate of the Fura2 fluorescence that was quenched by Mn^{2+} in wild-type, heterozygous, and homozygous myotubes from *RYR1*-p.G2435R mice after changing from imaging buffer to manganese buffer. (*B*) Box plots showing the quench rate (median and interquartile range) in control, 25 μM gadolinium–treated, or 250 nM SAR7334–treated myotubes from each of the three genotypes. The *whiskers* represent the 10th to 90th percentile. A larger rate of quench is represented by a more negative number, and this indicates a greater cationic entry through the sarcolemmal cation channels into the cell from the extracellular space, which is an estimate of the sarcolemmal permeability to Ca^{2+}. §$P < 0.05$ in *RYR1*-p.G2435R homozygous *versus RYR1*-p.G2435R heterozygous and wild-type mice. **$P < 0.005$ and ****$P < 0.0001$ in each genotype (Kruskal–Wallis test with Dunn's multiple comparisons test, N ≥ 35 myotubes for each condition).

malignant hyperthermia episode comes from and is maintained by sarcoplasmic reticulum Ca^{2+} stores. Based on our studies in other animal models relevant to malignant hyperthermia, we have previously suggested that sarcolemmal cation entry channels are, at the very least, significant contributors to the chronically elevated intracellular calcium in quiescent malignant hyperthermia muscles and myotubes[21,22] and that they play a similarly significant role during a fulminant malignant hyperthermia episode.[22]

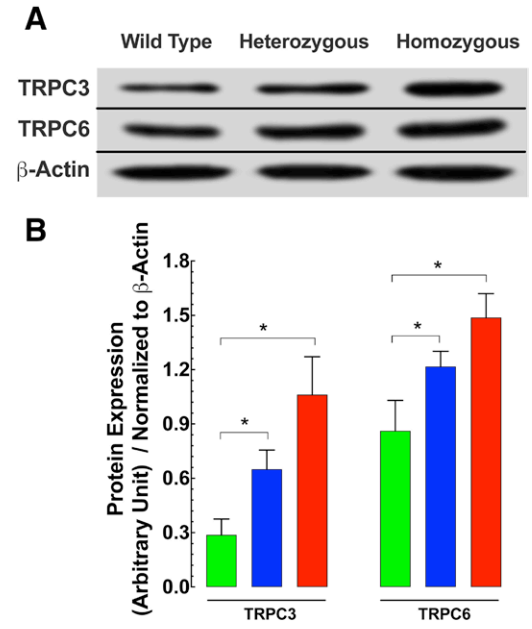

Fig. 8. (*A*) Representative Western blots showing the expression of TRPC3, TRPC6, and β-actin in wild-type, *RYR1*-p.G2435R heterozygous, and *RYR1*-p.G2435R homozygous gastrocnemius muscles. (*B*) Densitometric analysis of five independent Western blots for each transient receptor potential cation protein. The data were normalized to β-actin and are expressed as means ± SD. $N_{muscles}$ = 8; Student's unpaired independent *t* test. *$P \leq 0.05$.

A primary finding was that in addition to increased resting intracellular calcium, resting intracellular sodium is also elevated in *RYR1*-p.G2435R muscle cells (homozygous greater than heterozygous) compared with wild-type muscle cells, both *in vitro* and *in vivo*.[21,22] This suggests that at least one source of Ca^{2+} could be the extracellular pool and not the sarcoplasmic reticulum. In this study, we confirmed this hypothesis, showing that incubation of muscle with gadolinium, a potent nonspecific inhibitor of sarcolemmal cation influx, significantly reduced the intracellular levels of sodium and calcium and blocked manganese quench, a monitor of sarcolemmal cation entry.

Di-acyl-glycerol is a second messenger involved in key cellular processes in skeletal muscle and other excitable cells.[27] In addition to its role as a lipid second messenger to recruit protein kinases C, it also activates the di-acyl-glycerol–sensitive TRPC3/6 subgroup of transient receptor potential cation channels in the sarcolemma.[24,28] Here we utilized the membrane-permeable di-acyl-glycerol analog, 1-oleoyl-2-acetyl-*sn*-glycerol to determine whether the pathway for sarcolemmal sodium and calcium influx was through TRPC3 and TRPC6.[29,30] 1-Oleoyl-2-acetyl-*sn*-glycerol induced an elevation in the resting intracellular calcium and sodium in all three genotypes, and this was greater in *RYR1*-p.G2435R (greater in homozygous than heterozygous) muscle than wild-type muscle (figs. 2, A and B). The elevation of intracellular calcium and the increase rate of manganese quench elicited by 1-oleoyl-2-acetyl-*sn*-glycerol was blocked either by removal of extracellular Ca^{2+} or by blocking sarcolemmal Ca^{2+} and Na^{+} entry with gadolinium or SAR7334 (figs. 3, 4, and 6). These data rule out any possibility that 1-oleoyl-2-acetyl-*sn*-glycerol increased intracellular calcium by releasing Ca^{2+} from intracellular stores and confirmed that the source of the increase was through TRPC3/6, whose expression we showed was upregulated in *RYR1*-p.G2435R compared with wild-type muscles.

Incubation of wild-type and *RYR1*-p.G2435R muscle fibers with SAR7334, a much more specific blocker of TRPC6 and TRPC3 channels than gadolinium,[25] reduced resting calcium in *RYR1*-p.G2435R cells (in homozygous cells less than heterozygous cells, which have less than wild-type cells) and blocked the effects of 1-oleoyl-2-acetyl-*sn*-glycerol. Local application of SAR7334 directly to the superficial muscle fibers *in vivo* reduced resting intracellular calcium in homozygous *RYR1*-p.G2435R fibers and partially inhibited the halothane-induced increase in intracellular calcium in *RYR1*-p.G2435R muscle cells. This finding in particular demonstrates that during the malignant hyperthermia episode, there is an initial sarcoplasmic reticulum–supported increase in intracellular calcium that appears to be quickly partially depleted, as demonstrated by the rapid fall in intracellular calcium from ~750 to ~400 nM in the SAR7334-treated leg during the same time intracellular calcium rose to 1,373 ± 81 nM and then plateaus in the nontreated leg. All of these data together support the hypothesis that sarcolemmal Ca^{2+} entry plays a critical role in maintaining the new intracellular calcium steady state that has been observed during a malignant hyperthermia crisis. Furthermore, the observed immediate elevation of intracellular calcium in the SAR7334-treated leg is most probably mediated by Ca^{2+} release from the sarcoplasmic reticulum, and the decline in the intracellular calcium in this leg shows that that this level cannot be maintained by sarcoplasmic reticulum Ca^{2+} cycling because of Ca^{2+} extrusion and blockade of sarcolemmal Ca^{2+} entry.

Consistent with the 1-oleoyl-2-acetyl-*sn*-glycerol-mediated elevation of intracellular calcium and sodium in muscle cells plus the ability of the transient receptor potential cation channel-specific blocker SAR7334 to block both the pharmacologic and halothane-induced increase in Ca^{2+}, we also demonstrated that hyperforin, an activator of TRPC6 mediated inward cationic current,[26,31,32] mimicked the action of 1-oleoyl-2-acetyl-*sn*-glycerol, and its effect was greater in *RYR1*-p.G2435R (greater in homozygous than in heterozygous mice) than wild-type muscle cells. As observed with 1-oleoyl-2-acetyl-*sn*-glycerol, removal of extracellular Ca^{2+} also eliminated the hyperforin-elicited increase in resting intracellular calcium.[31] The enhanced cation flux observed across the sarcolemma in

RYR1-p.G2435R cells is consistent with the cell boundary theorem stating that the long-term steady state of the free intracellular calcium concentration inside cells must be driven by changes with the outside through fluxes across the plasmalemma.[22,33]

In summary, these results demonstrated that skeletal muscles of mice expressing the *RYR1*-p.G2435R mutation have an elevated resting intracellular calcium and sodium and a significantly enhanced, extracellular Ca^{2+} dependent response to 1-oleoyl-2-acetyl-*sn*-glycerol and hyperforin. We further showed that the 1-oleoyl-2-acetyl-*sn*-glycerol response could be prevented by TRPC3 and TRPC6 blockers. These results provide further support to our working hypothesis that in response to partial depletion of sarcoplasmic reticulum calcium stores caused by malignant hyperthermia causing mutations in RyR1, TRPC3 and TRPC6 channels play a critical role in producing the intracellular calcium and sodium overload both at rest and during the malignant hyperthermia crisis.

Research Support

Supported by National Institute of Arthritis, Musculoskeletal and Skin Diseases grant Nos. 1R01AR068897-01A1 (Bethesda, Maryland; to Drs. Allen, Hopkins, Rafael Lopez, and Liu) and 2P01 AR-05235 (to Drs. Allen, Rafael Lopez, and Hopkins), by Medical Research Council grant No. N002407/1 (London, United Kingdom; to Drs. Kaura, Hopkins, and Allen), and AFM-Téléthon-France grant No. 21543 (Evry, France; to Dr. Rafael Lopez).

Competing Interests

The authors declare no competing interests.

Correspondence

Address correspondence to Dr. Allen: Malignant Hyperthermia Investigation Unit, St. James' University Hospital, Leeds, United Kingdom. p.d.allen@leeds.ac.uk.

References

1. Nelson TE: Malignant hyperthermia: A pharmacogenetic disease of Ca^{++} regulating proteins. Curr Mol Med 2002; 2:347–69
2. Jurkat-Rott K, Lerche H, Lehmann-Horn F: Skeletal muscle channelopathies. J Neurol 2002; 249:1493–502
3. Groom L, Muldoon SM, Tang ZZ, Brandom BW, Bayarsaikhan M, Bina S, Lee HS, Qiu X, Sambuughin N, Dirksen RT: Identical *de novo* mutation in the type 1 ryanodine receptor gene associated with fatal, stress-induced malignant hyperthermia in two unrelated families. Anesthesiology 2011; 115:938–45
4. Parness J, Bandschapp O, Girard T: The myotonias and susceptibility to malignant hyperthermia. Anesth Analg 2009; 109:1054–64
5. Litman RS, Rosenberg H: Malignant hyperthermia: Update on susceptibility testing. JAMA 2005; 293:2918–24
6. Robinson R, Carpenter D, Shaw MA, Halsall J, Hopkins P: Mutations in RYR1 in malignant hyperthermia and central core disease. Hum Mutat 2006; 27:977–89
7. Yang T, Riehl J, Esteve E, Matthaei KI, Goth S, Allen PD, Pessah IN, Lopez JR: Pharmacologic and functional characterization of malignant hyperthermia in the R163C RyR1 knock-in mouse. Anesthesiology 2006; 105:1164–75
8. Chelu MG, Goonasekera SA, Durham WJ, Tang W, Lueck JD, Riehl J, Pessah IN, Zhang P, Bhattacharjee MB, Dirksen RT, Hamilton SL: Heat- and anesthesia-induced malignant hyperthermia in an RyR1 knock-in mouse. FASEB J 2006; 20:329–30
9. Lopez JR, Kaura V, Diggle CP, Hopkins PM, Allen PD: Malignant hyperthermia, environmental heat stress, and intracellular calcium dysregulation in a mouse model expressing the p.G2435R variant of RYR1. Br J Anaesth 2018; 121:953–61
10. Du GG, Sandhu B, Khanna VK, Guo XH, MacLennan DH: Topology of the Ca^{2+} release channel of skeletal muscle sarcoplasmic reticulum (RyR1). Proc Natl Acad Sci U S A 2002; 99:16725–30
11. Miller DM, Daly C, Aboelsaod EM, Gardner L, Hobson SJ, Riasat K, Shepherd S, Robinson RL, Bilmen JG, Gupta PK, Shaw MA, Hopkins PM: Genetic epidemiology of malignant hyperthermia in the UK. Br J Anaesth 2018; 121:944–52
12. Robinson RL, Brooks C, Brown SL, Ellis FR, Halsall PJ, Quinnell RJ, Shaw MA, Hopkins PM: RYR1 mutations causing central core disease are associated with more severe malignant hyperthermia *in vitro* contracture test phenotypes. Hum Mutat 2002; 20:88–97
13. Carpenter D, Robinson RL, Quinnell RJ, Ringrose C, Hogg M, Casson F, Booms P, Iles DE, Halsall PJ, Steele DS, Shaw MA, Hopkins PM: Genetic variation in RYR1 and malignant hyperthermia phenotypes. Br J Anaesth 2009; 103:538–48
14. López JR, Alamo L, Caputo C, DiPolo R, Vergara S: Determination of ionic calcium in frog skeletal muscle fibers. Biophys J 1983; 43:1–4
15. Lopez JR, Alamo LA, Jones DE, Papp L, Allen PD, Gergely J, Sréter FA: $[Ca^{2+}]_i$ in muscles of malignant hyperthermia susceptible pigs determined *in vivo* with Ca^{2+} selective microelectrodes. Muscle Nerve 1986; 9:85–6
16. Yang T, Esteve E, Pessah IN, Molinski TF, Allen PD, López JR: Elevated resting $[Ca^{2+}]_i$ in myotubes expressing

malignant hyperthermia RyR1 cDNAs is partially restored by modulation of passive calcium leak from the SR. Am J Physiol Cell Physiol 2007; 292:C1591–8
17. Eltit JM, Bannister RA, Moua O, Altamirano F, Hopkins PM, Pessah IN, Molinski TF, López JR, Beam KG, Allen PD: Malignant hyperthermia susceptibility arising from altered resting coupling between the skeletal muscle L-type Ca^{2+} channel and the type 1 ryanodine receptor. Proc Natl Acad Sci U S A 2012; 109:7923–8
18. Feng W, Barrientos GC, Cherednichenko G, Yang T, Padilla IT, Truong K, Allen PD, Lopez JR, Pessah IN: Functional and biochemical properties of ryanodine receptor type 1 channels from heterozygous R163C malignant hyperthermia-susceptible mice. Mol Pharmacol 2011; 79:420–31
19. López JR, Allen PD, Alamo L, Jones D, Sreter FA: Myoplasmic free [Ca^{2+}] during a malignant hyperthermia episode in swine. Muscle Nerve 1988; 11:82–8
20. Yuen B, Boncompagni S, Feng W, Yang T, Lopez JR, Matthaei KI, Goth SR, Protasi F, Franzini-Armstrong C, Allen PD, Pessah IN: Mice expressing T4826I-RYR1 are viable but exhibit sex- and genotype-dependent susceptibility to malignant hyperthermia and muscle damage. FASEB J 2012; 26:1311–22
21. Altamirano F, Eltit JM, Robin G, Linares N, Ding X, Pessah IN, Allen PD, López JR: Ca^{2+} influx via the Na^+/Ca^{2+} exchanger is enhanced in malignant hyperthermia skeletal muscle. J Biol Chem 2014; 289:19180–90
22. Eltit JM, Ding X, Pessah IN, Allen PD, Lopez JR: Nonspecific sarcolemmal cation channels are critical for the pathogenesis of malignant hyperthermia. FASEB J 2013; 27:991–1000
23. Yang T, Allen PD, Pessah IN, Lopez JR: Enhanced excitation-coupled calcium entry in myotubes is associated with expression of RyR1 malignant hyperthermia mutations. J Biol Chem 2007; 282:37471–8
24. Hofmann T, Obukhov AG, Schaefer M, Harteneck C, Gudermann T, Schultz G: Direct activation of human TRPC6 and TRPC3 channels by diacylglycerol. Nature 1999; 397:259–63
25. Maier T, Follmann M, Hessler G, Kleemann HW, Hachtel S, Fuchs B, Weissmann N, Linz W, Schmidt T, Löhn M, Schroeter K, Wang L, Rütten H, Strübing C: Discovery and pharmacological characterization of a novel potent inhibitor of diacylglycerol-sensitive TRPC cation channels. Br J Pharmacol 2015; 172:3650–60
26. Leuner K, Kazanski V, Müller M, Essin K, Henke B, Gollasch M, Harteneck C, Müller WE: Hyperforin: A key constituent of St. John's wort specifically activates TRPC6 channels. FASEB J 2007; 21:4101–11
27. Bouron A, Chauvet S, Dryer S, Rosado JA: Second messenger-operated calcium entry through TRPC6. Adv Exp Med Biol 2016; 898:201–49
28. Gudermann T, Hofmann T, Mederos y Schnitzler M, Dietrich A: Activation, subunit composition and physiological relevance of DAG-sensitive TRPC proteins. Novartis Found Symp 2004; 258:103–22, 155–9, 263–6
29. Tu P, Kunert-Keil C, Lucke S, Brinkmeier H, Bouron A: Diacylglycerol analogues activate second messenger-operated calcium channels exhibiting TRPC-like properties in cortical neurons. J Neurochem 2009; 108:126–38
30. Lemos VS, Poburko D, Liao CH, Cole WC, van Breemen C: Na^+ entry via TRPC6 causes Ca^{2+} entry via NCX reversal in ATP stimulated smooth muscle cells. Biochem Biophys Res Commun 2007; 352:130–4
31. Leuner K, Li W, Amaral MD, Rudolph S, Calfa G, Schuwald AM, Harteneck C, Inoue T, Pozzo-Miller L: Hyperforin modulates dendritic spine morphology in hippocampal pyramidal neurons by activating Ca^{2+}-permeable TRPC6 channels. Hippocampus 2013; 23:40–52
32. Treiber K, Singer A, Henke B, Müller WE: Hyperforin activates nonselective cation channels (NSCCs). Br J Pharmacol 2005; 145:75–83
33. Ríos E: The cell boundary theorem: A simple law of the control of cytosolic calcium concentration. J Physiol Sci 2010; 60:81–4